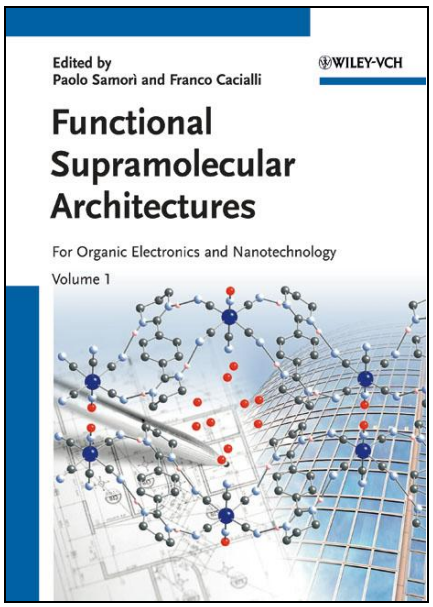

Samori, P. / Cacialli, F. (eds.)

Functional Supramolecular Architectures

for Organic Electronics and Nanotechnology

Description:

A comprehensive overview of functional nanosystems based on organic and polymeric materials and their impact on current and future research and technology in the highly interdisciplinary field of materials science. As such, this handbook covers synthesis and fabrication methods, as well as properties and characterization of supramolecular architectures. Much of the contents are devoted to existing and emerging applications, such as organic solar cells, transistors, diodes, nanowires and molecular switches. The result is an indispensable resource for materials scientists, organic chemists, molecular physicists and electrochemists looking for a reliable reference on this hot topic.

Reviews:

"Overall, I have thoroughly enjoyed reading these two volumes and believe that they will provide both an introduction to the field for the novel adepts who are starting to develop an interest in supramolecular chemistry and materials, as well as a useful guidance and a reference text, from fundamental to applications, for experts who would like to keep abreast of the field with the latest and most significant achievements for several years to come." (Materials Views, 13 September 2011)

"All in all, Functional Supramolecular Architectures is an excellent interdisciplinary resource for chemists, material scientists, and chemical engineers practicing in both academic and industrial R&D settings. In addition, it may be an intriguing choice as a primary text for a graduate-level special topics course dealing with functional supramolecular materials and applications thereof." (Journal of the American Chemical Society, 16 May 2011)

WILEY WILEY-BLACKWELL

18
Optical Properties and Electronic States in Anisotropic Conjugated Polymers: Intra- and Interchain Effects

Davide Comoretto, V. Morandi, M. Galli, F. Marabelli, and C. Soci

18.1
Introduction

In recent years, the implementation of organic semiconductors as active materials has led to the development of a new class of optoelectronic devices [1]. This was made possible by advancements in both synthesis of novel materials and experimental tools to investigate their properties. After the discovery of a dramatic variation of the conductivity of *trans*-polyacetylene upon doping [2], the synthesis of polymers such as polythiophenes, poly(*p*-phenylenes), poly(*p*-phenylene vinylenes), polyfluorenes, and their derivatives and copolymers possessing functional side groups has driven the flourishing of cost-effective organic light-emitting diodes (OLEDs), field-effect transistors (OFETs), photovoltaic cells (PVs), and sensors. On the other hand, the improved processability of conjugated polymers with high photo- and electroluminescence quantum yields has also enabled studying the complicated interplay of electron–phonon coupling and electron correlation in organic semiconductors. At present, the control of the supramolecular structure of polymeric macromolecules is an important research issue. While the nature of primary photoexcitation in conjugated polymers was initially discussed in the framework of isolated chains, it is now accepted that intermolecular interactions must be considered to understand in detail the electronic excited states of these systems. In spite of the rushing development of the field, many issues related to intermolecular interactions are still unclear, for instance, their influence on carrier photogeneration and carrier transport (mobility and lifetime), which are two crucial issues to the operation of OFETs and OPVs [3–6].

From the chemical point of view, intermolecular interactions control the supramolecular structure of molecular systems through noncovalent or secondary bonds, resulting in a variety of possible structures that range from simple molecular dimers to single crystals, J-aggregates, or mesophases [7–10]. Moreover, even in the amorphous phase or in solutions, conjugated polymers might be affected by the specific packing of their skeleton induced by thermal treatment and solution processing [6, 11–14].

Functional Supramolecular Architectures. Edited by Paolo Samori and Franco Cacialli

ISBN: 978-3-527-32611-2

The random coil conformation of macromolecules hinders the intrinsic anisotropy of π-electronic states. In spin-coated and drop-cast films, the preferential alignment of the polymer chains in the plane of the substrate often results in slight uniaxiality and optical anisotropy, with the ordinary refractive index lying in the plane of the substrate and the extraordinary refractive index lying perpendicularly [15–17]. However, large anisotropy is observable only in highly oriented materials, in which the macromolecules are chain extended and aligned, such as freestanding films oriented by tensile drawing [18]. In such oriented samples, the mechanical, electrical, and optical properties become more and more anisotropic as the degree of chain alignment and chain extension is increased [19–22].

In the following, we will review some recent studies on highly oriented PPV films. PPV and its substituted soluble derivatives are among the most widely studied conjugated polymers as they show both good photoluminescence and charge transport properties [23, 24]. Moreover, the availability of high-quality, well-oriented PPV samples [25–27] enabled to clarify some fundamental issues such as the assignment of the polarized optical transitions and the determination of the anisotropic dielectric functions [15, 16, 28–30]. This knowledge is essential to eliminate spurious effects in spectra obtained with nonconventional polarized spectroscopies, which may directly probe intra- and intermolecular interactions. The effects of intermolecular interactions on the electronic properties of conjugated polymers can be directly investigated with optical spectroscopies under hydrostatic pressure. Through the use of advanced optical models and polarized spectroscopy on oriented samples, the anisotropy of the electronic structure can be addressed [31, 32]. Despite the pioneering studies in the high-pressure field conducted in the 1980s with unoriented polymers and oligomers [33–37], a large amount of studies have recently focused on the optical, structural, conformational, and transport properties of oligomer and polymer single crystals under pressure [38–54].

Given the importance of polymer orientation to access the intrinsic anisotropy of the electronic properties, we will discuss this topic in Section 18.2. In Section 18.3, we will disentangle intrachain from interchain properties: while the former are primarily affected by conjugation length and chemical substitution, the latter are controlled by the supramolecular structure. In Section 18.4, we will report on polarized photoluminescence spectra, which show evidence of both intra- and interchain effects. The latter are ultimately probed by optical spectroscopy under hydrostatic pressure adopted to modulate the intermolecular distances and thus directly tune the strength of interchain interactions.

18.2
Polymer Properties and Orientation

Conventional plastic materials are electrical insulators. This is due to the presence of saturated σ-bonds between sp^3 hybridized carbon atoms in the polymer backbone. In insulating polymers, electronic transitions occur only for photon energies above 7 eV [55]. On the other hand, the sp^2 hybridization of the carbon atoms in

polyconjugated systems creates an alternation of single and double bonds that lowers the transition energies to values typical of semiconductors (1.5–4 eV). For few conjugated polymers, that is, polydiacetylene and polyline derivatives, sp hybridization gives rise to a CC triple bonds.

The differences between conjugated and nonconjugated polymers are related to both the electronic and macromolecular properties. Nonconjugated polymers are usually constituted by a large number of repeating units and are very flexible, thus easily processable from melt or solution. Conversely, conjugated polymers are stiff due to the presence of delocalized π-electrons, which reduce twisting around the C−C bonds, and are also responsible for the semiconducting properties. Conjugated polymers are usually not soluble or processable without adding proper side chains or dopants. Moreover, the total chain length and molecular weight distribution, characteristics that confer plastic properties, strongly depend on the synthetic route [56–59]. π-Electrons in conjugated polymers are rarely delocalized along the whole macromolecule, as the presence of chain twisting, branching, and defects reduces the delocalization to discrete molecular segments whose extension is called conjugation length (L_C). Conjugated segments having different L_C coexist within the same macromolecule, and each segment can be modeled as a modified infinite quantum well whose absorption energy is a function of $1/L_C$ [60–63]. L_C values and their distribution are strongly related to disorder, which determines the inhomogeneous broadening of electronic transitions and Raman modes. In amorphous or disordered polymers, inhomogeneous broadening smears out the vibronic progression of the pure electronic transitions [60, 64, 65]. Photoexcitation processes are also affected by disorder: the distribution of L_C affects energy migration as probed by site-selective fluorescence [66], while residual catalyst or oxygen might affect charge generation [67–70] or exciton migration [66]. In addition, macromolecular aggregation and supramolecular structure are affected by chain conformation, and increase for flat rod-like macromolecules and reduce for coil-like ones. Finally, additional synthetic issues such as regioregularity [14, 59, 71, 72], isomerization [73], phase transitions [74], and polymorphism [75] also affect the supramolecular structure. All these considerations point out the need for high-quality, ordered materials to understand the role of intermolecular interactions and, as a consequence, the photophysics of polymer systems.

Polarizability of π-electrons is extremely high along the polymer backbone, but it is orders of magnitude lower in the perpendicular direction. Unfortunately, the synthesis of conjugated polymers yields samples with randomly distributed macromolecules, in which the intrinsic anisotropy of the electronic properties is obscured. Consequently, oriented samples would be expected to display a strong anisotropy of the electronic and optical responses. Nevertheless, in some polymers, high-energy parallel and perpendicularly polarized optical transitions may have comparable intensities due to the specific orbitals involved [25–28, 76]. In addition, even weak interchain interactions could provide some extent of intermolecular polarization. Therefore, the identification of all these contributions is often not trivial and is further complicated by the fact that intermolecular effects could be easily masked by chain misalignment, which projects the large oscillator strength of the optical transitions polarized along the backbone into different directions [77].

Orientation of conjugated polymers is a demanding task for which several approaches have been attempted. The simpler method consists in the growth of single crystals [78–83], similar to what is actively pursued with small molecules to obtain large carrier mobilities for OFETs [84]. Unfortunately, single crystals of conjugated polymers are available only for few selected polydiacetylenes(PDAs) due to their peculiar polymerization mechanism [85]. Optical measurements on PDAs single crystals show a very high degree of anisotropy [86]. Recently, this polymerization mechanism has been refined to obtain isolated PDA chains embedded in their monomer single crystal with anisotropy of the π–π^* transition exceeding 50. These samples allowed the study of the single polymeric chain intrinsic anisotropy and novel optical effects [86–90].

A different approach to prepare oriented conjugated polymers consists in using vacuum evaporation on suitable substrates to induce epitaxy of the molecule to be oriented. For PDAs and oligothiophenes, very interesting results have been obtained on potassium acid phthalate single-crystal substrates [91–95]. Good orientation can also be achieved covering the substrate with a preoriented friction-transferred film of Teflon [96, 97]. This technique provides high-absorption dichroism (i.e., high orientation), but is applicable only to small molecules since the evaporation process is unsuitable for polymers with large molar mass. Despite the promising results obtained for PDAs, the above-mentioned orientation techniques are not applicable to the other families of conjugated polymers, for which different methods have been employed, such as Langmuir–Blodgett technique [98] and shearing in solutions [99, 100], in liquid crystal solutions [101, 102], or by directional solidification [103]. However, the degree of orientation achievable by these methods is often relatively poor and unsuitable for a detailed investigation of the anisotropic electronic properties.

A technique suitable to orient several polymer families is rubbing [104–106]. Rubbed substrates have also been successfully used to promote orientation of conjugated polymers cast over them. With this method, improved carrier mobility in liquid crystalline poly(9,9-di-*n*-octylfluorene-altbenzothiadiazole) (F8BT)-based FET have been obtained [84, 107]. Rubbing has also been directly applied to the emitting layer of OLEDs to achieve polarized emission [108–110]. Despite the technological interest raised by these remarkable results, the degree of anisotropy achieved is still insufficient for detailed fundamental studies on the anisotropic electronic or optical response, due to the presence of a large amount of misaligned polymeric chains [111, 112]. Relevant improvements of the orientation have been reported by matching the interaction between few families of molecules (diacetylenes and phenylene ethynylene) and the substrate by combining rubbing with the evaporation on preoriented Teflon layers [113].

A method yielding good orientation to almost every class of conjugated polymers is tensile drawing (stretching). When applied to insoluble conjugated polymers, tensile drawing provides good results, as in the case of Shirakawa's polyacetylene [77]. A better degree of orientation is achieved for nonconjugated polymer precursors, which can be converted after orientation, such as for Durham–Graz polyacetylene [114] or for PPV sulfonium precursor [115, 116]. In this case, conversion to the conjugated

form in suitable conditions allows retaining optimal polymer orientation [28, 31, 32, 76, 117–121]. Soluble conjugated polymers can optionally be blended in a host matrix, such as ultrahigh molecular weight polyethylene (UHMW-PE), before stretching. The orientation of the matrix induces orientation of the conjugated polymer guest and large dichroic ratios can be achieved [122–124]. The main drawback of this technique for optical studies is light scattering caused by the matrix in the blue and ultraviolet spectral regions [122–124]. One way to overcome this limitation is to coat the films with decane (a PE oligomer) to smoothen the corrugation induced by stretching. Refractive index matching reduces light scattering and allows the study of the optical anisotropy even in the UV spectral region [25–27].

18.3
Intrachain Effects

PPV freestanding films oriented by precursor tensile drawing (elongation ratio 4–5) [115, 125, 126] have proven to be an excellent system for modeling the anisotropic optical properties of highly oriented conjugated polymers. The large degree of ordering achieved in these samples has been confirmed by structural studies revealing the presence of crystallites packed in a herringbone pattern surrounded by amorphous regions [127, 128]. Figure 18.1 shows the polarized reflectance (R) and transmittance (T) spectra of stretch-oriented, freestanding PPV films over a wide spectral range. Note that hereafter the light polarization is referred to the orientation direction of the macromolecules [115, 116]. The orientation process induces a very large anisotropy of the optical response. Moreover, this system is very

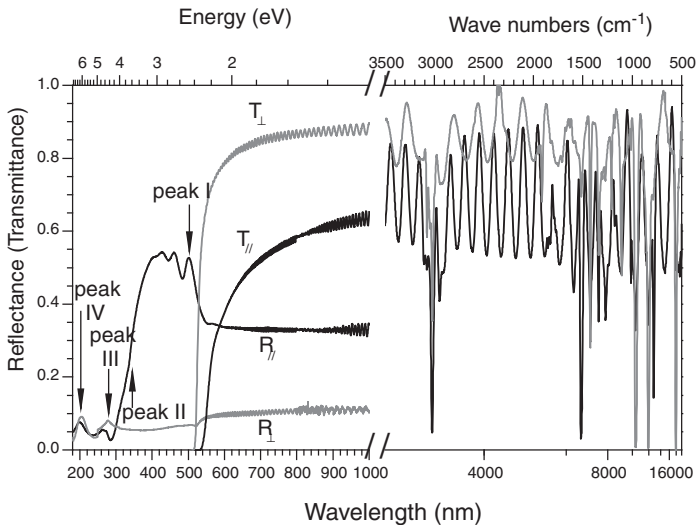

Figure 18.1 Polarized reflectance (R) and transmittance (T) spectra of highly oriented PPV (black line: || polarization; gray line: ⊥ polarization). Peaks I–IV indicate the main optical transitions in PPV.

well ordered as indicated by the resolved vibronic progressions observed for parallel polarization, which contrasts with usual PPV data, where the distribution of conjugation lengths smears out these fine structures [56, 60, 67, 105, 129]. The large degree of orientation is also confirmed by vibrational modes anisotropy in the medium infrared spectral region. The presence in all spectra of anisotropic interference fringe patterns due to Fabry–Perot multiple reflections at the surfaces highlights the optical quality of oriented films and again its optical anisotropy. Unfortunately, the interference pattern hampers a detailed identification of infrared vibrations [130–133], although no signature of carbonyl groups is detected even after several months of exposure to laboratory conditions, confirming the chemical stability of these samples and then their reliability for photophysical studies.

The assignment of electronic transitions observed in the absorption spectra of PPV and its derivatives has been long debated, partly due to limitations of the early theoretical models and the lack of high-quality samples that allowed accessing the intrinsic anisotropy of the electronic properties as well as of the dielectric functions [134, 135]. The availability of polarized optical spectra of highly oriented PPV [28, 31, 32, 76, 117–121] and its soluble derivatives [25, 26] provided a deeper insight into the nature of the optical transitions and was used to validate theoretical models [29, 105, 136–152]. Four main transitions are visible in Figure 18.1. For the parallel component, a strong signal associated with the π–π^* purely electronic transition of the lowest absorption band is observed at 2.48 eV (peak I), followed by a well-resolved vibronic progression with peaks at 2.70 and 2.95 eV and by a shoulder at 3.10 eV. Note that in unoriented PPV films, the π–π^* transition is found around 3 eV and depending on the synthetic route used [56], the shape of the vibronic progression is usually inhomogeneously broadened [60, 129, 153, 154] due to a broad L_C distribution; this is not the case of highly oriented PPV samples. The change in the slope of the spectrum around 3.76 eV indicates the presence of an additional transition (peak II). On the high-energy side of the spectrum, a low-intensity peak is observed at 4.71 eV accompanied by a shoulder at 4.56 eV (peak III). The lowest optical transition and its vibronic satellites cannot be detected in the perpendicular component of the reflectance spectrum. This implies that the polymer chains are very well oriented and misalignment is negligible. For the perpendicular component, a peak is observed at 4.47 eV (peak III). A fourth transition whose polarization is not well defined is observed at 6.08 eV (peak IV) [28, 76, 117–119]. Kramers–Kroenig analysis of these data and spectroscopic ellipsometry and interferometric techniques applied to similar samples led to the detailed determination of the anisotropic dielectric functions of PPV [28, 155]. Since the dielectric functions are directly correlated to the electronic structure of the material, the comparison with theoretical data enables the assignment of the optical transitions.

The experimental data are comparable to the results of quantum chemical calculations for 15-ring PPV oligomers, which allow establishing the origin of the various peaks [28, 76]. The fine structure observed in peak I derives from the π–π^* transition followed by a vibronic progression that can be described within the Franck–Condon approximation. Peak III originates from the $l \rightarrow d^*/d \rightarrow l^*$ transition involving localized (l) and delocalized (d) states [28, 105]. This transition has

a dominant polarization perpendicular to the chain axis. Peak IV results from $l \rightarrow l^*$ excitations (localized at *para*-position of phenyl rings) and is predicted to be polarized parallel to the chain axis. In agreement with the experimental data, calculations also suggest that the shoulder observed in the reflectance spectrum of unsubstituted PPV around 3.7 eV (peak II) corresponds to an optical transition between delocalized levels ($d \rightarrow d^*$), which is induced by finite-size effects (i.e., the ends of conjugated segments) and is polarized along the chain axis. The intensity of this peak decreases when L_C is increased [28, 105].

To better understand the assignment of optical transition in PPV, it is interesting to compare the data of oriented PPV to those of PPV derivatives such as poly[2-methoxy-5-(2′-ethyl-hexyloxy)-1,4-phenylene vinylene] (MEH-PPV) and poly[2-butyl-5-(2′-ethyl-hexyl)-1,4-phenylene vinylene] (BuEH-PPV). The polarized absorption data of oriented PPV, MEH-PPV, and BuEH PPV films are shown in Figure 18.2 [25, 26]. These films are stretch oriented after blending the conjugated polymer

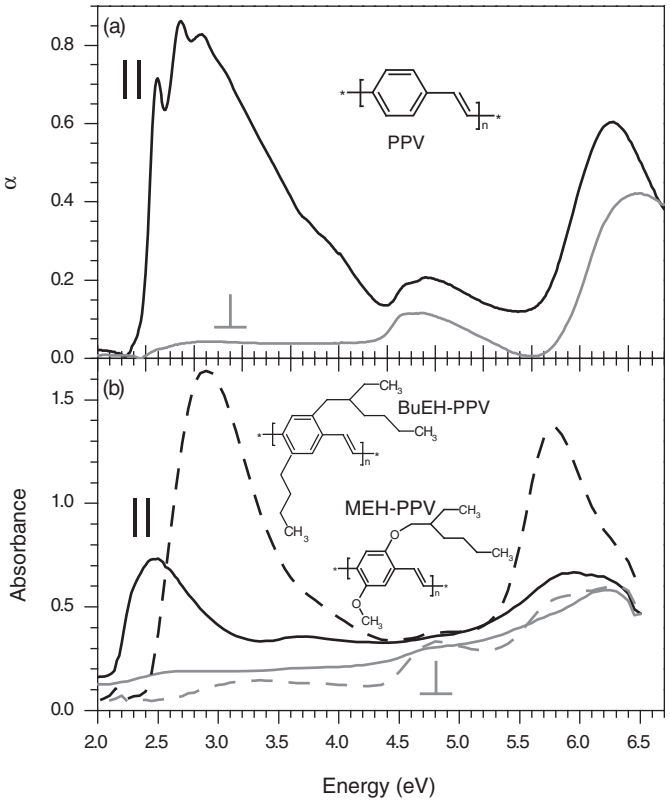

Figure 18.2 Comparison of polarized (parallel: black, perpendicular: gray) absorption spectra of oriented PPV and its derivatives. (a) Pristine PPV. (b) MEH-PPV (solid line) and BuEH-PPV (dashed line). Spectra in (b) are adapted from Ref. [25, 26]. Chemical structures of the polymers are shown in the insets.

with UHMW-PE. Alkoxy-substituted derivatives [25] are characterized by a large intensity of peak II at 3.7 eV (Figure 18.2b), which appears as a shoulder in PPV. The main effect of the alkoxy groups is indeed to decrease the separation between the energies of the lowest $l \rightarrow d^*/d \rightarrow l^*$ and $d \rightarrow d^*$ excitations, thus enhancing the strength of the interaction among them. This causes an intensity redistribution from the π–π^* transition to peak II, which is therefore expected to increase in intensity. Interestingly, quantum chemical calculations show that the transition dipole moment of these new peaks is almost exclusively governed by their weak $d \rightarrow d^*$ character (i.e., the contributions of the $l \rightarrow d^*/d \rightarrow l^*$ excitations tend to cancel each other), which settles their polarization along the chain axis [28, 105]. It was also shown that by increasing L_C, the intensity of peak II decreases due to the larger separation between l and d excitations, which reduces transfer of oscillator strength from the π–π^* transition [28, 105]. In oriented PPV (Figure 18.2a), both peak I and peak II are polarized parallel to the chain axis. However, in these samples, peak II has a vanishingly small intensity due to the wide extension of L_C [105].

The relative intensity of peak II varies among the three polymers. When side groups are electronically inactive (e.g., in PPV and BuEH-PPV), peak II appears as a weak shoulder. On the other hand, the intensity of peak II increases considerably in MEH-PPV where the conjugated backbone is directly linked to electroactive oxygen atoms. The presence of peak II in PPV and BuEH-PPV (Figure 18.2b) implies the existence of a second mechanism that has been related to finite-size effects by theoretical calculations [28, 76, 105, 117–120, 137, 152, 156, 157]. They predict that the combination of these two effects in substituted PPV derivatives yields a transition with the correct parallel polarization, while the rupture of charge conjugation symmetry alone would give rise to a transition with perpendicular polarization, inconsistent with the experimental results [105, 137, 140, 142–144].

Additional differences between PPV derivatives concern peak I. While in the spectrum of PPV the 0–0 transition at 2.5 eV shows a well-resolved vibronic progression, in MEH-PPV and BuEH-PPV the vibronic structure is smeared out by the distribution of effective L_C. In MEH-PPV, the 0–0 transition energy is likely to coincide with the shoulder that appears around 2.3 eV. This corresponds to a redshift of 0.2 eV induced by the substitution of the conjugated backbone, as predicted by theoretical calculations [139]. In BuEH-PPV, a blueshift of π–π^* transition to $\sim$2.9 eV is observed, probably due to a reduced average L_C in this material. The narrower distribution of effective conjugation lengths in PPV compared to that prevailing in substituted derivatives indicates a larger intramolecular order, which has the potential to affect intermolecular interactions, morphologies, and phases. In turn, all these effects may alter the picture of the electronic properties of isolated chains so far considered. For instance, MEH-PPV, in spite its long substituents, has a crystalline structure [150, 158], which is very different from that observed for PPV [127, 128], thus inducing remarkable differences in the photophysics of the two polymers. Such effects are not uncommon to conjugated polymer systems [32, 77, 121, 159, 160].

Further considerations can be made by comparing the width of the lowest optical transition and the vibronic progression in the three polymers. The full width at half maximum (FWHM) increases from 0.67 eV in MEH-PPV to 0.85 eV in BuEH-PPV

and 1.13 eV in PPV. Since in oriented PPV the inhomogeneous broadening due to intramolecular effects and disorder is reduced and since backbones are more closely packed than in its substituted derivatives due to the absence of steric hindrance between lateral chains [127], the different FWHM observed in the spectra in Figure 18.2 suggests a correlation between the optical properties and the polymer supramolecular structure.

18.4 Interchain Effects

Despite the massive work reported on the orientation of conjugated macromolecules [25–27, 110, 114, 124, 161–167], a general understanding of the processes underlying their electro-optical response has not yet been achieved. For instance, recent studies on the optical properties of unoriented PPV derivatives have questioned the character of the emitting excitons (i.e., intrachain versus interchain), indicating that intermolecular interactions, both in solution [168] and in silica nanoparticle composites [153, 169], may significantly affect the absorption [158, 170] and emission spectra [171]. A comparison between the absorption and photoluminescence properties of highly oriented PPV samples with those of unoriented samples is helpful for further understanding of these issues. To this purpose, the detailed knowledge of the polymer optical constants and their anisotropy is required [28, 172–174]. Indeed, a meaningful interpretation of polarized PL spectra requires the correction of the emission spectra for equal number of absorbed (exciting) photons, as well as for self-absorption, refraction, and reflectivity losses. The details concerning the determination of the PPV optical properties and the optical model used to correct the raw photoluminescence PL data are reported elsewhere [32]; here we will briefly discuss the origin of these corrections and focus on the derived PL data with particular emphasis on their anisotropies.

18.4.1 Polarized Photoluminescence Spectra

Figure 18.3a shows the corrected PL spectra of oriented PPV films for the various polarization configurations of the excitation/detection at room temperature. The correction factors modify the shape of PL spectra as well as the relative magnitude of the peak intensities. Due to the highly anisotropic optical properties of oriented PPV, these factors strongly depend on the experimental configuration of polarizations and are larger where the dispersion of the refractive index is high, (e.g., on the high-energy side of the PL spectra). The low-energy side of the correction factors is weakly dispersive and, since the sample is transparent in this region, it is mainly due to the different reflectivity for each given configuration of the polarizations. The largest correction factor corresponds to the (||, ||) configuration, where the emission suffers the highest losses due to the high reflection of the excitation as well as of the emission

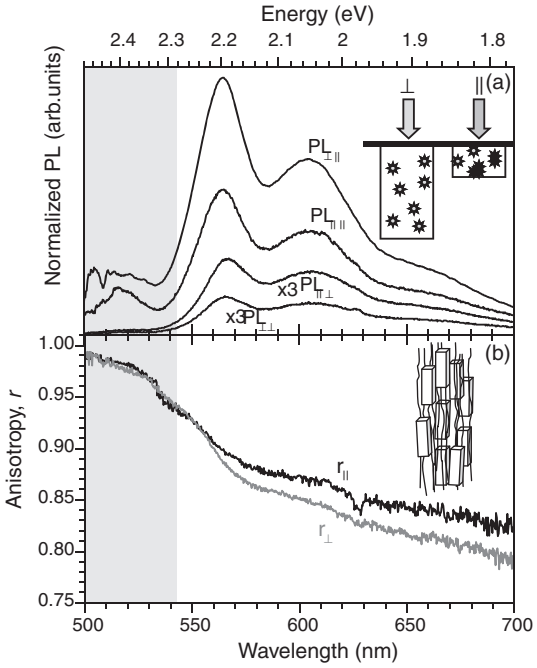

Figure 18.3 (a) PL spectra for different combination of pump/emission polarizations after the corrections described in Ref. [32]. *Inset*: Sketch of the pump polarization anisotropy effect. Arrows indicate the exciting radiation, open stars the emitting centers, and dark stars the quenched centers. (b) Spectral response of the anisotropy function *r* for parallel and perpendicular polarization of the excitation. The inset is a sketch of the morphology of oriented PPV according to Ref. [127]. Shaded area highlights emission polarized along the chain axis.

at the polymer–air interface, while the smallest correction applies to the (⊥, ⊥) configuration where reflection of both excitation and emission is lower [32].

After correction, (||, ||) and (⊥, ||) PL spectra at room temperature show a well-defined peak at 520 nm, which resembles the 0–0 transitions detected in the PL spectra of thin PPV films [169, 175]. For the remaining configurations (||, ⊥ and ⊥, ⊥), there is no clear evidence for any additional structure underneath the high-energy tail of the main emission peak. Note that upon lowering the temperature, the PL signal intensity increases by a factor greater than 3 and peaks in the PL spectra shift toward longer wavelength (517 → 530 nm; 565 nm → 573 nm; 605 nm → 618 nm) [32]. Moreover, the main PL peaks are unusually broadened at low temperature, suggesting an energy-level splitting induced by weak intermolecular interactions. To the best of our knowledge, the anomalous broadening of PL bands upon lowering the temperature was never observed before, and points to the effect of intermolecular interactions on the emission properties as also suggested by studies of PPV/silica nanocomposites [169, 175].

18.4.1.1 Pump Polarization Anisotropy

The intensity of the PL spectra derived for excitation polarized perpendicular to the draw axis results to be almost twice the one derived for excitation parallel polarized, independent of the emission polarization (Figure 18.3a) [32]. This effect, referred to as "pump polarization anisotropy," has been previously observed in the photoconductive response and photoinduced absorption of different polymers [77, 160, 176–178]. Pump polarization anisotropy is typical of thick films and can be understood in terms of photogenerated species quenching. In the case of oriented PPV films, excitons are quenched by charge carriers as supported by the high charge photogeneration efficiency, the lack of stimulated emission, and the relatively low PL quantum efficiency (2–5%) [32, 179]. For parallel excitation polarization, the small absorption depth due to the large absorption coefficient ($\lambda_{||} \sim 1/\alpha_{||} \sim 10$ nm) results in a relatively high concentration of excitations near the sample surface that increases the probability of exciton quenching and reduces the PL signal (Figure 18.3a, inset). On the other hand, due to the weaker absorption, the light penetration depth is significantly larger for perpendicular excitation polarization ($\lambda_{\perp} \sim 1/\alpha_{\perp} \sim 100\,\lambda_{||}$), thus the probability of exciton quenching is strongly reduced (Figure 18.3a, inset). Due to the reduced emitter density, quenching is poorly active and thus a larger PL intensity is expected for perpendicular rather than for parallel polarization of the excitation. Note that this effect is expected only in optically thick films, that is, films where the thickness (d) is $d \gg 1/\alpha$. In optically thin films, where the penetration depth for both polarizations is larger than d, the (||, ||) component of the PL is still expected to be the most intense due to the larger emission dipole moment along the chain axis [180].

18.4.2 Emission Anisotropy

The PL emission anisotropy is well described by the orientation function r for a given pump polarization (parallel or perpendicular to the polymer chain orientation):

$$r_{||} = \frac{\mathrm{PL}_{||,||} - 2PL_{||,\perp}}{\mathrm{PL}_{||,||} + 2PL_{||,\perp}} \quad \text{or} \quad r_{\perp} = \frac{\mathrm{PL}_{\perp,||} - 2PL_{\perp,\perp}}{\mathrm{PL}_{\perp,||} + 2PL_{\perp,\perp}} \tag{18.1}$$

Equation 18.1 is calculated with corrected PL intensities for parallel or perpendicular excitation (Figure 18.3a). The spectral dependence of r obtained for parallel and perpendicular excitation is displayed in Figure 18.3b. As expected, the anisotropy is almost independent of the excitation route. However, the strong spectral dependence of the orientation functions is evident, with almost complete polarization of the high-energy emission peak (shaded area in Figure 18.3) along the polymer chain axis ($r > 0.99$) and considerably lower polarization of the low-energy structures ($r \sim 0.85$). The dependence of the orientation function on the emission wavelength, with crossover at about 540 nm, suggests a different origin of the emitting states responsible for the high-energy (520–530 nm) and the low-energy peaks (530–700 nm) of the PL. This conclusion is further supported by the different temperature dependence of the high- and low-energy PL peaks as well as by the increased broadening of the PL spectra upon lowering the temperature [32].

A possible explanation of this effect is the presence of "defects" acting as a sink for the excitations and providing an alternative de-excitation pathway to the standard intramolecular radiative decay. The high energy part of the PL spectrum, with intrinsic anisotropy comparable to that of the absorption, could be assigned to an intramolecular decay, while the low energy part to a "defect"-mediated decay. In the case of stretch-oriented PPV films, the origin of such "defect" may relate to the presence of crystalline (70% of the volume) and amorphous regions (Figure 18.3b inset) [181]. Within each crystallite (∼20 nm size), chains are packed in an orthorhombic structure with intermolecular separations of either 5 Å (translational periodicity along the *b*-axis) or 3.9 Å (between benzene ring layers in the unit cell). Even though the highest interchain coupling is predicted to take place in the cofacial arrangement, such small intermolecular separations can allow significant interactions [158]. Thus, the two emitting states inferred from the analysis of the emission anisotropy may be attributed to the amorphous and crystalline phases coexisting in the oriented PPV samples. In the amorphous phase, the electronic transitions mainly stem from isolated macromolecules (emitting at higher energies), while in the crystalline phase, intermolecular interactions would affect the electronic structure, reducing the energy gap and thus lowering the emission energy. In this case a reduced anisotropy is expected.

18.4.3
Polarized Optical Spectroscopy under Hydrostatic Pressure

Hydrostatic pressure was used to directly control the intermolecular interactions in highly oriented PPV. Since the pioneering work on polyacetylenes [34] and polydiacetylenes [33, 35–37], the investigation of spectroscopic properties under hydrostatic pressure has become a powerful tool to probe the properties of conjugated polymers. When a polymer is subject to an external applied pressure, several effects occur simultaneously. From an intramolecular point of view, pressure induces a planarization of backbones, a phenomenon that has been extensively investigated by X-ray diffraction and vibrational spectroscopy [38, 47, 51, 182, 183]. In general, planarization induces an increase of the conjugation length, which in turn causes a redshift of absorption and emission spectra [39–41, 47]. Besides intrachain effects, applied pressure changes the interchain separation and favors the overlapping of wavefunctions belonging to different macromolecules. The increment of the interaction between adjacent chains brought closer together is of fundamental importance. Despite the interactions along the polymer chain that are dominant and determine the main optical and electronic properties of organic semiconductors, 3D effects can dramatically alter the 1D picture and its photophysics, thus improving both charge photogeneration and transport [184, 185].

Two main effects are typically observed in optical spectra under an applied pressure: the redshift of transition energies and the broadening of transition linewidths [39, 54, 129]. In conjugated polymers, however, these changes may be irrespectively attributed to interchain or to intrachain effects. Indeed, polymers are usually weakly ordered materials, and the distinct observation of intermolecular

interactions is hampered by both the random distribution of polymeric chains and their conformations. In disordered systems, flattening of the backbone chains is mainly responsible for the observed redshift and the effects of intra- and intermolecular interactions are not easily unraveled. In a recent paper [186], the pressure-induced redshift of the PL spectrum of F8BT was compared to that of a solid-state solution of the same polymer. From the difference between the redshift observed in the latter, where interchain coupling is negligible due to the large chain separation, and the one in thin film, it was possible to isolate the contribution due to interchain coupling.

It is important to note that el–ph coupling is not negligible in weakly ordered systems and determines an overall broadening of the electronic and vibronic transitions [31, 185]. The order of the system, therefore, becomes crucial to distinguish intramolecular from intermolecular contributions. Molecular crystals are good examples. Here, several terms contribute to the energy of an exciton: the excitation energy of the free molecule, the solvent shift, the exciton shift, and the Davydov splitting [35, 187]. The study of the compressibility of polydiacetylene crystals showed that the pressure shift of the absorption is essentially due to an increase of the gas-to-crystal shift term under pressure [33], while the solvent shift is related to the mean value of the bulk modulus [35]. Pressure-induced structural changes in crystalline oligo(paraphenylenes) with a different number of phenyl rings also showed that changes in intermolecular distances and molecular arrangement have a relevant effect on bulk properties [182]. The bulk modulus was found to depend linearly on the inverse number of phenyl rings in the molecules and on their density in ambient condition. Finally, we note that the Davydov splitting is usually neglected in polymeric samples since disorder masks its optical fingerprint. As a matter of fact, it was unambiguously observed only for a unique species of PDA single crystals where a well-known phase transition giving rise to a doubling of the number of chains within the crystalline cell occurs [188].

Polarized spectroscopy under pressure was used to study highly oriented PPV to highlight the role of intermolecular interactions. Here, we will not present the methodologies adopted for the complicated optical data reduction, which are elsewhere described [31, 189], but we show and discuss the resulting polarized Raman and reflectivity spectra.

18.4.3.1 Raman Spectroscopy

Raman spectra ($\lambda_{exc} = 632.8$ nm) of highly oriented PPV have been recorded up to 30 kbar. At atmospheric pressure, five main Raman modes are clearly detectable at 1170 cm^{-1} (C−H bending of the phenyl ring), 1329 cm^{-1} (C=C stretching + CH bending of the vinyl group), 1548 cm^{-1} (C=C phenyl stretching), 1583 cm^{-1} (C−C phenyl stretching), and 1627 cm^{-1} (C=C vinyl stretching) [31]. The assignment of these modes is well established [129, 130, 190], and no other bands appear in the Raman spectrum by applying pressure.

It is interesting to compare the pressure-dependent Raman data of oriented PPV with those of PPV oligomers and unoriented PPV films [39, 54]. It has been previously observed that the ratio between the intensities of the C−H bending of the phenyl

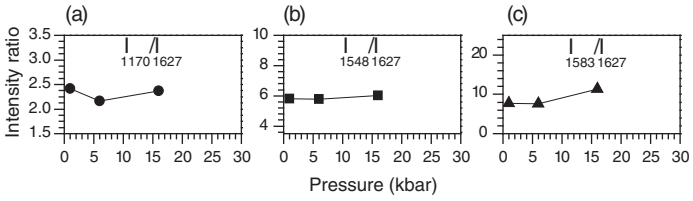

Figure 18.4 Pressure dependence of Raman mode intensity ratios of highly oriented PPV. (a) I_{1170}/I_{1627}. (b) I_{1548}/I_{1627}. (c) I_{1583}/I_{1627}.

ring, C=C phenyl stretching, and C−C phenyl stretching to that of C=C vinyl stretching of PPV oligomers increases upon increasing their length, thus such ratios are good probe of the L_C extension [129, 191]. By this argument, Raman spectroscopy can be used to evaluate the geometrical changes (flattening) of the polymer structure induced by hydrostatic pressure. The pressure dependence of the relative intensity of Raman modes (I_{1170}/I_{1627}, I_{1548}/I_{1627}, I_{1583}/I_{1627}) in oriented PPV is shown in Figure 18.4. Noticeably all ratios are almost independent of pressure up to 16 kbar. While in unoriented PPV, I_{1543}/I_{1622} was found to grow from 1 to 2.4 upon increasing the applied pressure up to 80 kbar [39], in oriented PPV, I_{1543}/I_{1622} equals 2.4 already at atmospheric pressure and does not increase at higher pressure. Since the ratio I_{1543}/I_{1622} is proportional to the extension of L_C, this indicates that in stretch-oriented PPV, L_C is considerably high and is almost independent of applied pressure, while in unoriented PPV, large conjugation lengths can be achieved only at high applied pressures. Similar arguments have been previously applied to the study of other conjugated polymers, including ladder-type poly(*p*-phenylene), F8BT derivatives, and *para*-hexaphenyl [47, 50, 183, 186, 192]. These observations point out to the fact that oriented PPV is highly planar and has exceedingly large conjugation length, which can hardly be improved by applying pressure. Therefore, any effect of hydrostatic pressure on the linear optical properties of highly oriented PPV has to be regarded as nearly independent of intrachain ordering (planarization).

18.4.3.2 **Reflectance Spectroscopy**

The reflectance spectra of oriented PPV measured for different applied pressures with light polarization parallel to the polymer chains are shown in Figure 18.5a. At atmospheric pressure, the π–π^* transition is located at 2.46 eV (504 nm). Well-resolved vibronic replicas are also observed at 2.70, 2.90, and 3.09 eV (460, 427, and 401 nm).

The overall effect of pressure on the parallel component of R is a rigid redshift of the entire spectrum together with a considerable broadening of all electronic transitions as well as their vibronic replicas. Since intramolecular effects (increased L_C), as probed by Raman spectroscopy, are negligible, the pressure dependence of the π–π^* transition must originate from a different mechanism, that is, the strengthening of intermolecular interactions. Figure 18.5b shows the perpendicular component of the reflectance spectra for different applied pressures. These spectra are

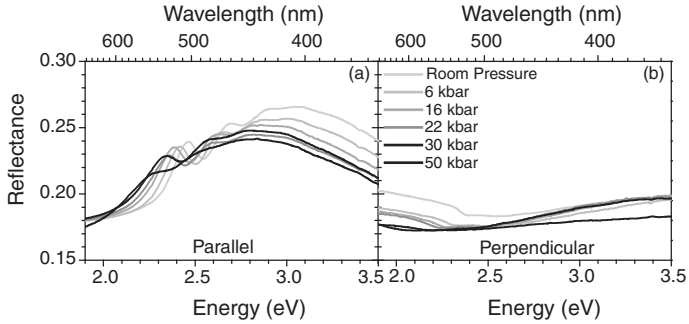

Figure 18.5 Reflectance spectra of PPV for different applied pressures. (a) Parallel polarization. (b) Perpendicular polarization.

almost structureless due to the very good orientation of the polymeric chains. Only minor details due to residual misalignment can be recognized [31].

Knowledge of the complex dielectric function ($\varepsilon_1 + i\varepsilon_2$) is again a key issue to interpret the pressure dependence of reflectance data. Since the narrow spectral range and the uncertainties in modeling the interface between the sample and the diamond culet hinder the use of Kramers–Kronig (K–K) transformations or ellipsometry, a fitting procedure based on a series of K–K consistent Gaussian oscillators was used to derive the components of the complex dielectric constant from the data in Figure 18.5 [189]. To reproduce accurately the π–π^* transition and each vibronic replica, two Gaussian functions instead of one were necessary even for the spectra at atmospheric pressure. As already observed for R spectra, the ε_1 and ε_2 spectra obtained by such procedure show broadening and bathochromic shift when pressure is applied [189]. Figure 18.6 shows the pressure dependence of the peak energy, area, and width of the two Gaussians used to fit the purely electronic 0–0 transition. By increasing applied pressure, the requirement of two Gaussians becomes more stringent and can be interpreted as evidence of energy-level splitting due to intermolecular interactions. As a matter of fact, upon applying pressure, the doublet necessary to reproduce the structure clearly splits into two peaks separated by $\sim$110 meV at 50 kbar (Figure 18.6a). Concurrently, the area underneath the lower energy peak increases with pressure and becomes comparable with the area underneath the higher energy peak at 50 kbar (Figure 18.6b). Moreover, both

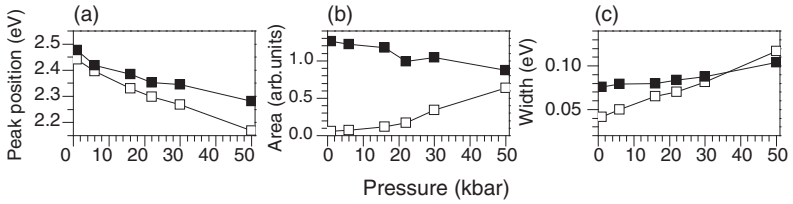

Figure 18.6 Pressure dependence of the fitting parameters corresponding to peak positions (a), areas (b), and width (c) of transitions responsible for the 0–0 peak. Empty (solid) squares refer to the lowest (highest) energy component of each doublet.

Gaussians broaden at higher pressures, as shown by the pressure dependence of the width parameters (Figure 18.6c).

From these observations we conclude that at atmospheric pressure, the 0–0 transition is mostly due to the high-energy peak. On the other hand, when chains are brought closer to each other, the strength of the lower energy peak increases at the expense of the higher energy one. The splitting occurring between the two components might be interpreted as the Davydov splitting caused by the peculiar crystal symmetry of highly oriented PPV, with two nonequivalent chains per unit cell. Theoretical calculations of the optical properties of crystalline PPV predict a Davydov splitting of ~120 meV [158], consistent with our data where a variation from 35 to 113 meV is observed in the investigated pressure range. Broadening of all the vibronic transitions upon applied pressure can be attributed to the enhanced interchain interactions. A contribution to the broadening from a change in the el–ph coupling upon changing pressure was also suggested [31].

18.4.3.3 **Oscillator Strength**

The overall influence of pressure on ε is remarkably different for the parallel and perpendicular polarization. Upon applying pressure, the overall intensity of the parallel component of ε_2 decreases. Conversely, the perpendicular component of ε_2 increases in intensity with pressure, showing a strong enhancement for energies higher than 2.4 eV [189]. More detailed information on the electronic structure of oriented PPV can be obtained by analyzing the oscillator strength for parallel and perpendicular polarized transitions.

Within the quantum theory of absorption and dispersion, the sum rule for the oscillator strength of optical transitions in a solid is given by [193, 194]

$$\left(\frac{m}{2\pi^2 N_C e^2}\right) \int_0^{\omega_x} \omega\varepsilon_2(\omega)\mathrm{d}\omega = f(\omega_x) \tag{18.2}$$

where N_C is the carbon atom density (16 atoms in an orthorhombic crystallographic cell $8.07 \times 5.08 \times 6.54$ Å^3) [128], e is the electronic charge, m is the electronic mass, and ω is the frequency. Equation 18.2 relates the imaginary part of the dielectric constant to the oscillator strength f of the optical response within the frequency ω_x. The dispersion curves of the oscillator strength for oriented PPV with parallel and perpendicular polarization as well as for an isotropic PPV system are reported in Figure 18.7. Figure 18.7a clearly shows that for the parallel polarization, the oscillator strength is conserved up to 2.75 eV (451 nm), although it is spectrally redistributed due to the broadening and splitting previously discussed. For photon energies above 2.75 eV, the oscillator strength decreases upon applying pressure. In the case of perpendicular polarization, however, the oscillator strength increases upon increasing applied pressure (Figure 18.7b). Since the overall oscillator strength should be conserved, we deduce that oscillator strength must transfer from the parallel to the perpendicular polarization, particularly in the highest energy range. This is indeed observed when looking at the isotropic oscillator strength ($f_{ISO} = f_{\parallel} + 2f_{\perp}$) calculated

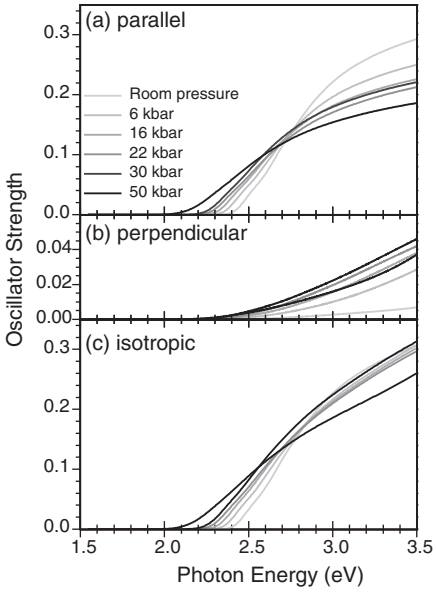

Figure 18.7 Oscillator strength derived by numerical integration of parallel (a), perpendicular (b), and isotropic (c) components of ε_2.

from the polarized components (Figure 18.7c). We believe this *f* transfer may be due to intermolecular interactions that increase the system dimensionality. At present, the microscopic mechanism underlying the oscillator strength transfer from the || to the $\perp$ component is not fully understood. It may stem from the presence of optical states that are almost dark at atmospheric pressure, but gain oscillator strength in the perpendicular polarization by increasing pressure. Alternatively, new optically allowed states may originate at high pressure from a phase transition within polymer crystallites. Comparison with theoretical calculations is very difficult since ε_2 spectra are reported only for molecular crystals based on fluorene [195] or *para*-terphenyl [53]. Calculations of the anisotropic imaginary components of the dielectric function or oscillator strength for conjugated polymers will be necessary to elucidate these points.

A final comment on f_{ISO} concerns the importance of oriented samples for these kinds of studies. Indeed, the anomalous transfer of oscillator strength from the || to the $\perp$ component could not be observed in isotropic samples where the parallel and orthogonal components of the optical response are mixed together.

18.5 Conclusions

Highly oriented conjugated polymers are unique systems to address fundamental yet open issues on the photophysics of organic semiconductors. Among the various alignment techniques reviewed, tensile drawing is the one suitable to align any kind

of polymers, with minimal chain misalignment and high optical quality. Thus, polymer films oriented by tensile drawing enable the investigation of the intrinsic anisotropy of their electronic structure via optical studies. The origin and polarization of the optical transitions in highly oriented PPV films and its substituted derivatives have been discussed. Polarized photoluminescence spectra of oriented PPV revealed the existence of two emitting species, one fully polarized along the stretching direction and the other with a strong perpendicular component. Combined with the unusual spectral broadening and spectral shifts of the low- and high-energy PL peaks upon lowering the temperature, these data have been interpreted in terms of the emission from intramolecular species characteristic of oriented chains in amorphous regions and intermolecular species characteristic of crystalline regions where macromolecules are packed in a highly ordered structure. This hypothesis has been corroborated by spectroscopic studies conducted under hydrostatic pressure, which allow controlling the intrinsic intermolecular separation. While in amorphous polymer systems, the effect of hydrostatic pressure typically increases the intramolecular order and the extension of L_C, in the case of highly oriented PPV Raman scattering, experiments indicate that the very long L_C is poorly increased by applied pressure. Therefore, the effects of pressure observed in the optical spectra are due to a different mechanism, that is, intermolecular interactions. From reflectance spectra, the polarized complex dielectric constant and its pressure dependence were derived. These spectra show that a Davydov splitting due to the interaction between inequivalent chains in the crystallographic cell occurs, although a contribution from el–ph interaction is observed. A detailed analysis of the oscillator strength shows that for parallel polarization, the electronic transitions below 2.75 eV redistribute their oscillator strength by broadening and splitting, while those at higher energies, lose oscillator strength. For perpendicular polarization, an increase of oscillator strength is observed in the investigated spectral range. This component gains intensity from the parallel one and was assigned to electronic states correlated to intermolecular interactions.

Acknowledgments

Many people contributed to this work with helpful discussions over the years. Among them we would like to acknowledge D. Moses, A.J. Heeger, K. Miller, J. Cornil, J.L. Bredas, S. Mazumdar, V. Vardeny, F. Spano, and A. Painelli. We are particularly grateful to D. Moses for providing the PPV samples used in our studies.

This research has been mainly supported by the Italian Ministry of Instruction, University and Research under FIRB project No. RBNE03S7XZ. V.M. acknowledges a grant from Regione Lombardia (project REGLOM16).

References

1 Nalwa, H.S. (ed.) (2001) *Handbook of Advanced Electronic and Photonic Materials and Devices*, vol. 8, Academic Press.

2 Chiang, C.K., Fincher, C.R., Park, Y.W. *et al.* (1977) *Phys. Rev. Lett.*, **39**, 1098.
3 Wang, Z., Mazumdar, S., and Shukla, A. (2008) *Phys. Rev. B*, **78**, 235109.
4 Psiachos, D. and Mazumdar, S. (2009) *Phys. Rev. B*, **79**, 155106.
5 Holt, J., Singh, S., Drori, T. *et al.* (2009) *Phys. Rev. B*, **79**, 195210.
6 Clark, J., Silva, C., Friend, R.H. *et al.* (2007) *Phys. Rev. Lett.*, **98**, 206406.
7 Ciferri, A. (2005) *Supramolecular Polymers*, CRC Press, Boca Raton, FL.
8 Kobayashi, T. (1996) *J-Aggregates*, World Scientific, Singapore.
9 Haziioannou, G. and Hutten, P.F.v. (1999) *Semiconducting Polymers*, Wiley-VCH Verlag GmbH, Weinheim.
10 deBoer, B., Stalmach, U., Nijland, H. *et al.* (2000) *Adv. Mater.*, **12**, 1581.
11 Nguyen, T.Q., Doan, V., and Schwartz, B.J. (1999) *J. Chem. Phys.*, **110**, 4068.
12 Kanemoto, K., Imanaka, Y., Akai, I. *et al.* (2007) *J. Phys. Chem.*, **B111**, 12389.
13 Gierschner, J., Mack, H.G., Luer, L. *et al.* (2002) *J. Chem. Phys.*, **116**, 8596.
14 McCullough, R.D. (1998) *Adv. Mater.*, **10**, 93.
15 Tammer, M. and Monkman, A.P. (2002) *Adv. Mater.*, **14**, 210.
16 Ramsdale, C.M. and Greenham, N.C. (2002) *Adv. Mater.*, **14**, 212.
17 Losurdo, M., Giangregorio, M.M., Capezzuto, P. *et al.* (2009) *Adv. Mater.*, **21**, 1.
18 Comoretto, D. and Lanzani, G. (2003) in *Organic Photovoltaic* (eds C.J. Brabec *et al.*), Springer, Berlin, p. 57.
19 Akagi, K., Suezaki, M., Shirakawa, H. *et al.* (1989) *Synth. Met.*, **28**, D1.
20 Tokito, S.Z., Smith, P., and Heeger, A.J. (1990) *Synth. Met.*, **36**, 183.
21 Tsutsui, T., Murata, H., Momii, T. *et al.* (1991) *Synth. Met.*, **41**, 327.
22 Bradley, D.D.C., Friend, R.H., Hartmann, T. *et al.* (1987) *Synth. Met.*, **17**, 473.
23 Burroughes, J.H., Bradley, D.D.C., Brown, A.R. *et al.* (1990) *Nature*, **347**, 539.
24 Braun, D. and Heeger, A.J. (1991) *Appl. Phys. Lett.*, **58**, 1982.
25 Miller, E.K., Yoshida, D., Yang, C.Y. *et al.* (1999) *Phys. Rev. B*, **59**, 4661.
26 Miller, E.K., Yang, C.Y., and Heeger, A.J. (2000) *Phys. Rev. B*, **62**, 6889.
27 Miller, E.K., Maskel, G.S., Yang, C.Y. *et al.* (1999) *Phys. Rev. B*, **60**, 8028.
28 Comoretto, D., Dellepiane, G., Marabelli, F. *et al.* (2000) *Phys. Rev. B*, **62**, 10173.
29 Moses, D., Wang, J., Heeger, A.J. *et al.* (2001) *Proc. Natl. Acad. Sci. USA*, **98**, 13496.
30 Losurdo, M., Bruno, G., and Irene, E.A. (2003) *J. Appl. Phys.*, **94**, 4923.
31 Morandi, V., Galli, M., Marabelli, F. *et al.* (2009) *Phys. Rev. B*, **79**.
32 Soci, C., Comoretto, D., Marabelli, F. *et al.* (2007) *Phys. Rev. B*, **75**.
33 Lochner, K., Bässler, H., Sowa, H. *et al.* (1980) *Chem. Phys.*, **52**, 179.
34 Moses, D., Feldblum, A., Ehrenfreund, E. *et al.* (1982) *Phys. Rev. B*, **26**, 3361.
35 Lacey, R.J., Batchelder, D.N., and Pitt, G.D. (1984) *J. Phys. C Solid State Phys.*, **17**, 4529.
36 Lacey, R.J., Williams, R.L., Kennedy, R.J. *et al.* (1981) *Chem. Phys. Lett.*, **83**, 65.
37 Hangyo, M., Itakura, K., Nakashima, S. *et al.* (1986) *Solid State Commun.*, **60**, 739.
38 Mårdalen, J., Cerenius, Y., and Haggkvist, P. (1995) *J. Phys. Condens. Matter*, **7**, 3501.
39 Webster, S. and Batchelder, D.N. (1996) *Polymer*, **37**, 4961.
40 Mårdalen, J., Samuelsen, E.J., Konestabo, O.R. *et al.* (1998) *J. Phys. Condens. Matter*, **10**, 7145.
41 Kaniowski, T., Niziol, S., Sanetra, J. *et al.* (1998) *Synth. Met.*, **94**, 111.
42 Samuelesen, E.J., Mardalen, J., Konestabo, O.R. *et al.* (1999) *Synth. Met.*, **101**, 98.
43 Fedorko, P. and Skakalova, V. (1998) *Synth. Met.*, **94**, 279.
44 Yang, G., Li, Y., White, J.O. *et al.* (1999) *J. Phys. Chem. B*, **103**, 5181.
45 Yang, G., Li, Y., White, J.O. *et al.* (1999) *J. Phys. Chem. B*, **103**, 7853.
46 Guha, S., Graupner, W., Resel, R. *et al.* (1999) *Phys. Rev. Lett.*, **82**, 3625.
47 Guha, S., Graupner, W., Yang, S. *et al.* (1999) *Phys. Status Solidi B*, **211**, 177.
48 Heimel, G., Puschnig, P., Cai, Q. *et al.* (2001) *Synth. Met.*, **116**, 163.
49 Mikat, J., Orgzall, I., and Hochheimer, H.D. (2001) *Synth. Met.*, **116**, 167.

50 Guha, S., Graupner, W., Resel, R. *et al.* (2001) *J. Phys. Chem. A*, **105**, 6203.
51 Zhuravlev, K.K. and McCluskey, M.D. (2001) *J. Phys. Chem.*, **114**, 5465.
52 Rothe, C., Hintschich, S.I., Palsson, L.-O. *et al.* (2002) *Chem. Phys. Lett.*, **360**, 111.
53 Puschnig, P., Hummer, K., Ambrosch-Draxl, C. *et al.* (2003) *Phys. Rev. B*, **67**, 235321.
54 Zeng, Q.G., Ding, Z.J., Tang, X.D. *et al.* (2005) *J. Lumin.*, **115**, 32.
55 Mort, J. and Pfister, G. (1982) *Electronic Properties of Polymers*, John Wiley & Sons, Inc, New York.
56 Halliday, D.A., Burn, P.L., Friend, R.H. *et al.* (1993) *Synth. Met.*, **55**, 954.
57 Babudri, F., Farinola, G.M., Naso, F. *et al.* (2007) *Chem Commun.*, 1003.
58 Babudri, F., Cardone, A., Farinola, G.M. *et al.* (2008) *Eur. J. Org. Chem.*, **11**, 1977.
59 Kiebooms, R., Menon, R., and Lee, K. (2001) in *Handbook of Advanced Electronic and Photonic Materials and Devices*, vol. 8 (ed. H.S. Nalwa), Academic Press.
60 Osterbacka, R., Wohlgenannt, M., Shkunov, M. *et al.* (2003) *J. Chem. Phys.*, **118**, 8905.
61 Wenz, G., Muller, M.A., Schmidt, M. *et al.* (1984) *Macromolecules*, **17**, 837.
62 Hoffmann, R., Janiak, C., and Kollmar, C. (1991) *Macromolecules*, **24**, 3725.
63 Gierschner, J., Cornil, J., and Egelhaaf, H.-J. (2007) *Adv. Mater.*, **19**, 173.
64 Scholes, G.D., Larsen, D.S., Fleming, G.R. *et al.* (2000) *Phys. Rev. B*, **61**, 13670.
65 Mulazzi, E., Botta, C., Facchinetti, D. *et al.* (2004) *Synth. Met.*, **142**, 85.
66 Baessler, H. (1997) in *Primary Photoexcitations in Conjugated Polymers: Molecular Excitation versus Semiconductor Band Model* (ed. N.S. Sariciftci), World Scientific, Singapore, p. 51.
67 Rothberg, L.J., Yan, M., Papadimitrakopoulos, F. *et al.* (1996) *Synth. Met.*, **80**, 41.
68 Yan, M., Rothberg, L.J., Papadimitrakopoulos, F. *et al.* (1994) *Phys. Rev. Lett.*, **72**, 1104.
69 Cumpston, B.H. and Jensen, K.F. (1998) *J. Appl. Polym. Sci.*, **69**, 2451.
70 Harrison, N.T., Hayes, G.R., Philipps, R.T. *et al.* (1996) *Phys. Rev. Lett.*, **77**, 1881.
71 Osterbacka, R., An, C.P., Jiang, X.M. *et al.* (2000) *Science*, **287**, 839.
72 Korovynako, O.J., Osterbacka, R., Jiang, X.M. *et al.* (2001) *Phys. Rev. B*, **64**, 235122.
73 Heeger, A.J. (2001) *Rev. Mod. Phys.*, **73**, 681.
74 Ariu, M., Lidzey, D.G., and Bradley, D.D.C. (2000) *Synth. Met.*, **111–112**, 607.
75 Lu, G.H., Li, L.G., and Yang, X.N. (2007) *Adv. Mater.*, **19**, 3594.
76 Comoretto, D., Dellepiane, G., Moses, D. *et al.* (1998) *Chem. Phys. Lett.*, **289**, 1.
77 Comoretto, D., Dellepiane, G., Musso, G.F. *et al.* (1992) *Phys. Rev. B*, **46**, 10041.
78 Weiser, G. and Möller, S. (2002) *Phys. Rev. B*, **65**, 045203.
79 Muccini, M., Lunedei, E., Bree, A. *et al.* (1998) *J. Chem. Phys.*, **108**, 7327.
80 Tavazzi, S., Besana, D., Borghesi, A. *et al.* (2002) *Phys. Rev. B*, **65**, 205403.
81 Tavazzi, S., Borghesi, A., Laicini, M. *et al.* (2004) *J. Chem. Phys.*, **121**, 8542.
82 Tavazzi, S., Borghesi, A., Papagni, A. *et al.* (2007) *Phys. Rev. B*, **75**, 245416.
83 Laicini, M., Spearman, P., Tavazzi, S. *et al.* (2005) *Phys. Rev. B*, **71**, 045212.
84 Sirringhaus, H., Tessler, N., and Friend, R.H. (1998) *Science*, **280**, 1741.
85 Bloor, D. and Chance, R.R. (1985) *Polydiacetylenes*, Nijhoff, Dordrecht.
86 Weiser, G. (1992) *Phys. Rev. B*, **45**, 14076.
87 Spagnoli, S., Berréhar, J., Lapersonne-Meyer, C. *et al.* (1994) *J. Chem. Phys.*, **100**, 6195.
88 Schott, M. (2003) *Synth. Met.*, **139**, 739.
89 Weiser, G. and Berrehar, J. (2007) *Phys. Rev. Lett.*, **99**, 196401.
90 Weiser, G., Berrehar, J., and Schott, M. (2007) *Phys. Rev. B*, **76**, 205201.
91 LeMoigne, J., Kajzar, F., and Thierry, A. (1991) *Macromolecules*, **24**, 2622.
92 Costa, V.D., Moigne, J.L., Ostwald, L. *et al.* (1998) *Macromolecules*, **31**, 1635.
93 Comoretto, D., Moggio, I., Dell'Erba, C. *et al.* (1996) *Phys. Rev. B*, **54**, 16357.
94 Borghesi, A., Sassella, A., Tubino, R. *et al.* (1998) *Adv. Mater.*, **10**, 931.
95 Sassella, A., Borghesi, A., Meinardi, F. *et al.* (2000) *Phys. Rev. B*, **62**, 11170.
96 Wittman, J.C. and Smith, P. (1991) *Nature*, **352**, 414.
97 Fahlman, M., Rasmusson, J., Kaeriyama, K. *et al.* (1994) *Synth. Met.*, **66**, 123.

98 Pedriali, R., Cuniberti, C., Comoretto, D. *et al.* (1996) *Thin Solid Films*, **284**, 36.
99 Thakur, M. and Meyler, S. (1985) *Macromolecules*, **18**, 2341.
100 Gason, S.J., Dunston, D.E., Smith, T.A. *et al.* (1997) *J. Phys. Chem. B*, **101**, 7732.
101 Sariciftci, N.S. (1997) *Synth. Met.*, **80**, 137.
102 Soci, C., Moses, D., Heeger, A.J. *et al.* (2006) *Jpn. J. Appl. Phys.*, **45**, L33.
103 Brinkmann, M. and Wittmann, J.-C. (2006) *Adv. Mater.*, **18**, 860.
104 Kajzar, F., Lorin, A., Moigne, J.L. *et al.* (1995) *Acta Physiol. Pol.*, **87**, 713.
105 Chandross, M., Mazumdar, S., Liess, M. *et al.* (1997) *Phys. Rev. B*, **55**, 1486.
106 Yang, C.Y., Soci, C., Moses, D. *et al.* (2005) *Synth. Met.*, **155**, 639.
107 Pichler, K., Friend, R.H., Burn, P.L. *et al.* (1993) *Synth. Met.*, **55**, 454.
108 Jandke, M., Strohriegl, P., Gmeiner, J. *et al.* (1999) *Adv. Mater.*, **11**, 1518.
109 Bolognesi, A., Botta, C., Facchinetti, D. *et al.* (2001) *Adv. Mater.*, **13**, 1072.
110 Grell, M. and Bradley, D.D.C. (1999) *Adv. Mater.*, **11**, 895.
111 Comoretto, D., Moggio, I., Cuniberti, C. *et al.* (1998) *Phys. Rev. B*, **57**, 7071.
112 Nagamatsu, S., Takashima, W., Kaneto, K. *et al.* (2003) *Macromolecules*, **36**, 5252.
113 Moggio, I., Moigne, J.L., Arias-Marin, E. *et al.* (2001) *Macromolecules*, **34**, 7091.
114 Leising, G. (1988) *Phys. Rev. B*, **38**, 10313.
115 Kuroda, S., Noguchi, T., and Ohnishi, T. (1994) *Phys. Rev. Lett.*, **72**, 286.
116 Ohnishi, T., Noguchi, T., Nakano, T. *et al.* (1991) *Synth. Met.*, **41**, 309.
117 Comoretto, D., Dellepiane, G., Marabelli, F. *et al.* (2001) *Synth. Met.*, **116**, 107.
118 Comoretto, D., Marabelli, F., Tognini, P. *et al.* (2001) *Synth. Met.*, **124**, 53.
119 Comoretto, D., Marabelli, F., Tognini, P. *et al.* (2001) *Synth. Met.*, **119**, 643.
120 Comoretto, D., Soci, C., Marabelli, F. *et al.* (2005) *Synth. Met.*, **153**, 281.
121 Soci, C., Moses, D., Xu, Q.H. *et al.* (2005) *Phys. Rev. B*, **72**.
122 Hagler, T.W., Pakbaz, K., Moulton, J. *et al.* (1991) *Polym. Commun.*, **32**, 339.
123 Hagler, T.W., Pakbaz, K., Voss, K.F. *et al.* (1991) *Phys. Rev. B*, **44**, 8652.
124 Hagler, T.W., Pakbaz, K., and Heeger, A.J. (1994) *Phys. Rev. B*, **49**, 10968.
125 Kuroda, S., Murase, I., Ohnishi, T. *et al.* (1987) *Synth. Met.*, **17**, 663.
126 Kuroda, S., Murata, K., Noguchi, T. *et al.* (1995) *J. Phys. Soc. Jpn.*, **64**, 1363.
127 Yang, C.Y., Lee, K., and Heeger, A.J. (2000) *J. Mol. Struct.*, **521**, 315.
128 Chen, D., Winokur, M.J., Masse, M.A. *et al.* (1992) *Polymer*, **33**, 3116.
129 Mulazzi, E., Ripamonti, A., Wery, J. *et al.* (1999) *Phys. Rev. B*, **60**, 16519.
130 Tian, B., Zerbi, G., and Mullen, K. (1991) *J. Chem. Phys.*, **95**, 3198.
131 Heun, S., Mahrt, R.F., Greiner, A. *et al.* (1993) *J. Phys. Condens. Matter*, **5** 247.
132 Hrenar, T., Mitric, R., Meic, Z. *et al.* (2003) *J. Mol. Struct.*, **661–662**, 33.
133 Honda, K., Furukawa, Y., and Nishide, H. (2006) *Vib. Spectrosc.*, **40**, 149.
134 Sariciftci, N.S. (1997) *Primary Photoexcitations in Conjugated Polymers: Molecular Exciton versus Semiconductor Band Model*, World Scientific, Singapore.
135 Skotheim, T.A., Elsembaumer, R.L., and Reynolds, J.R. (1998) *Handbook of Conducting Polymers*, Marcel Dekker, New York.
136 Kirova, N., Brazovskii, S., and Bishop, A.R. (1999) *Synth. Met.*, **100**, 29.
137 Kohler, A., dos Santos, D.A., Beljonne, D. *et al.* (1998) *Nature*, **392**, 903.
138 Chandross, M. and Mazumdar, S. (1997) *Phys. Rev. B*, **55**, 1497.
139 Cornil, J., dos Santos, D.A., Beljonne, D. *et al.* (1995) *J. Phys. Chem.*, **99**, 5604.
140 Fahlman, M., Logdlund, M., Stafstrom, S. *et al.* (1995) *Macromolecules*, **28**, 1959.
141 Gartstein, Y.N., Rice, M.J., and Conwell, E.M. (1995) *Phys. Rev. B*, **51**, 5546.
142 Gartstein, Y.N., Rice, M.J., and Conwell, E.M. (1995) *Phys. Rev. B*, **52**, 1683.
143 Rice, M.J. and Gartstein, Y.N. (1994) *Phys. Rev. Lett.*, **73**, 2504.
144 Cornil, J., Beljonne, D., Friend, R.H. *et al.* (1994) *Chem. Phys. Lett.*, **223**, 82.
145 Cornil, J., Beljonne, D., Shuai, Z. *et al.* (1995) *Chem. Phys. Lett.*, **247**, 425.
146 Cornil, J., Beljonne, D., Heller, C.M. *et al.* (1997) *Chem. Phys. Lett.*, **278**, 139.
147 Zojer, E., Shuai, Z., Leising, G. *et al.* (1999) *J. Chem. Phys.*, **111**, 1668.
148 Brédas, J.L., Cornil, J., and Heeger, A.J. (1996) *Adv. Mater.*, **8**, 447.

149 Beljonne, D., Cornil, J., Silbey, R. *et al.* (2000) *J. Chem. Phys.*, **112**, 4749.

150 Ferretti, A., Ruini, A., Molinari, E. *et al.* (2003) *Phys. Rev. Lett.*, **90**, 086401.

151 Van der Horst, J.-W., Bobbert, P.A., and Michels, M.A.J.M. (2002) *Phys. Rev. B*, **66**, 035206.

152 Brazovskii, S., Kirova, N., Bishop, A.R. *et al.* (1998) *Opt. Mater.*, **9**, 472.

153 Ho, P.K.H., Kim, J.S., Tessler, N. *et al.* (2001) *J. Chem. Phys.*, **115**, 2709.

154 Ho, P.K.H. and Friend, R.H. (2002) *J. Chem. Phys.*, **116**, 6782.

155 Galli, M., Marabelli, F., and Comoretto, D. (2005) *Appl. Phys. Lett.*, **86**.

156 Brazovskii, S., Kirova, N., and Bishop, A.R. (1998) *Opt. Mater.*, **9**, 465.

157 Ambrosch-Draxl, C. and Abt, R. (1997) *Synth. Met.*, **85**, 1099.

158 Ruini, A., Caldas, M.J., Bussi, G. *et al.* (2002) *Phys. Rev. Lett.*, **88**, 206403.

159 Comoretto, D., Dellepiane, G., Musso, G. *et al.* (1991) *Synth. Met.*, **43**, 3515.

160 Comoretto, D., Dellepiane, G., Cuniberti, C. *et al.* (1996) *Phys. Rev. B*, **53**, 15653.

161 Bradley, D.D.C., Shen, Y.Q., Bleier, H. *et al.* (1988) *J. Phys. C Solid State Phys.*, **21**, L515.

162 Virgili, T., Lidzey, D.G., Grell, M. *et al.* (2002) *Appl. Phys. Lett.*, **80**, 4088.

163 Liem, H.M., Etchegoin, P., Whitehead, K.S. *et al.* (2003) *Adv. Funct. Mater.*, **13**, 66.

164 Pichler, K., Halliday, D.A., Bradley, D.D.C. *et al.* (1993) *J. Phys. Condens. Matter*, **5**, 7155.

165 Hagler, T.W., Pakbaz, K.J., Voss, K.F. *et al.* (1991) *Phys. Rev. B*, **44**, 945.

166 Luzzati, S., Moggio, I., Comoretto, D. *et al.* (1998) *Synth. Met.*, **95**, 47.

167 Herz, L.M. and Phillips, R.T. (2000) *Phys. Rev. B*, **61**, 13691.

168 Nguyen, T.Q., Kwong, R.C., Thompson, M.E. *et al.* (2000) *Appl. Phys. Lett.*, **76**, 2454.

169 Hoffmann, M. and Soos, Z.G. (2002) *Phys. Rev. B*, **66**, 024305.

170 Pedersen, T.G. (2004) *Phys. Rev. B*, **69**, 075207.

171 Samuel, I.D.W., Rumbles, G., and Collison, C.J. (1995) *Phys. Rev. B*, **52**, 11573.

172 Kim, J.S., Ho, P.K.H., Greenham, N.C. *et al.* (2000) *J. Appl. Phys.*, **88**, 1073.

173 Campoy-Quiles, M., Etchegoin, P.G., and Bradley, D.D.C. (2005) *Phys. Rev. B*, **72**, 045209.

174 Wan, W.M.V., Greenham, N.C., and Friend, R.H. (2000) *J. Appl. Phys.*, **87**, 2542.

175 Park, S.-J., Choi, E.-S., Oh, E.-J. *et al.* (2001) *Synth. Met.*, **117**, 95.

176 Siddiqui, A.S. (1984) *J. Phys. C Solid State Phys.*, **17**, 683.

177 Yang, Y., Lee, J.Y., Jain, A.K. *et al.* (1991) *J. Phys. Condens. Matter*, **3** 9563.

178 Sinclair, M., Moses, D., Friend, R.H. *et al.* (1987) *Phys. Rev. B*, **36**, 4296.

179 Miranda, P.B., Moses, D., and Heeger, A.J. (2001) *Phys. Rev. B*, **64**, 081201.

180 Hayes, G.R., Samuel, I.D.W., and Phillips, R.T. (1997) *Phys. Rev. B*, **56**, 3838.

181 Sokolik, I., Yang, Z., Karasaz, F.E. *et al.* (1993) *J. Appl. Phys.*, **74**, 3584.

182 Heimel, G., Puschnig, P., Oehzelt, M. *et al.* (2003) *J. Phys. Condens. Matter*, **15**, 3375.

183 Chandrasekhar, M., Guha, S., and Graupner, W. (2001) *Adv. Mater.*, **13**, 613.

184 Brédas, J.L., Calbert, J.P., Filho, D.A.d.S. *et al.* (2002) *Proc. Natl. Acad. Sci.*, **99**, 5804.

185 Barford, W. (2005) *Electronic and Optical Properties of Conjugated Polymers*, Oxford University Press, Oxford.

186 Schmidtke, J.P., Kim, J.S., Gierschner, J. *et al.* (2007) *Phys. Rev. Lett.*, **99**, 167401.

187 Pope, M. and Swenberg, C.E. (1999) *Electronic Processes in Organic Crystals*, Oxford University Press, New York.

188 Nowak, M.J., Blanchard, G.J., Baker, G.L. *et al.* (1990) *Phys. Rev. B*, **41**, 7933.

189 Morandi, V., Galli, M., Marabelli, F. *et al.* *J. Appl. Phys.*, submitted.

190 Orion, I., Buisson, J.P., and Lefrant, S. (1998) *Phys. Rev. B*, **57**, 7050.

191 Tian, B., Zerbi, G., Schenk, R. *et al.* (1991) *J. Chem. Phys.*, **95**, 3191.

192 Yi, G.R., Manoharan, V.N., Klein, S. *et al.* (2002) *Adv. Mater.*, **14**, 1137.

193 Wooten, F. (1972) *Optical Properties of Solids*, Academic Press, New York.

194 Smith, D.Y. (1985) in *Handbook of Optical Constants of Solids* (ed. E.D. Palik), Academic Press, Orlando, p. 35.

195 Heimel, G., Hummer, K., Ambrosch-Draxl, C. *et al.* (2006) *Phys. Rev. B*, **73**, 024109.